Computational Methods for 3D Shape Modeling and Analysis in the Context of the Virtual Physiological Human

Giuseppe Patané and Michela Spagnuolo

Abstract Computer Graphics and mathematical methods provide effective solutions for modeling, analyzing, and classifying shapes with a relevant role in diagnosis, surgical treatments, and follow-up. In this context, this paper discusses a number of computational methods for modeling and analyzing the morphology of anatomic structures, their spatial features and relations. 3D reconstructions of anatomical structures are widely used for surgical interventions and are typically derived from medical images. To improve the data resolution and reduce morphological artifacts, we present local approximation methods that conjugate different features, such as approximation accuracy and extrapolation capabilities higher than linear precision methods; robustness with respect to data discretization; computational efficiency. These techniques are also useful for the generation of volumetric meshes for bio-mechanical simulations in orthopedics. Then, we discuss automatic and semi-automatic segmentation methods for identifying and delimitating elongated structures, such as blood vessels and muscles. These structures can be associated to their centerlines for supporting further inspections, through camera navigation and virtual surgery. Shape-based segmentation techniques also allow the construction of structural representations of the input data, built upon a multi-scale segmentation into main bodies (e.g., heart, muscles) and limb features (e.g., vessels). These decompositions and the corresponding skeletal representations naturally follow the shape and extent of the limb features. Finally, geometric and morphological parameters are extracted to further support a deeper and more accurate understanding of the underlying anatomy and pathologies. The integration of quantitative parameters extracted from multi-modality imaging techniques allows the generation of more accurate predictive models of normal and dysfunctional behavior of organs and tissues. This innovation is improved by the extraction of physiological parameters, which are then used to generate more accurate virtual models of normal and disease states. Finally, we present a method to extract the semantics underlying 3D

CNR-IMATI
Via De Marini 6, 16149 Genova – Italy,
e-mail: [patane,spagnuolo]@ge.imati.cnr.it

reconstructions with morphological parameters, which also supports the documentation and storage of important medical information together with the 3D geometry.

1 Introduction

Computational methods play a prominent role in supporting collaborative investigation of the human body, as foreseen by the Virtual Physiological Human framework, especially for supporting descriptive and predictive actions. This is particularly relevant for computational methods involving the processing of multi-dimensional data, the modeling of anatomical structures, and the simulation of complex physiological systems, such as the muscoloskeletal one. Computational methods developed in the context of Computer Graphics provide effective solutions for modeling medical data, for analyzing and classifying shapes with a relevant role in diagnosis, surgical treatments, and follow-up. These elements motivate our review and discussion of a number of computational methods for modeling and analyzing the morphology of anatomical structures, their spatial features and relations, together with their abstraction and the extraction of the underlying semantics.

Nowadays, medical data are acquired through different modalities such as computerized tomography, ultrasound, positron emission tomography, and magnetic resonance imaging. Among them, the magnetic resonance imaging provides the best compromise between versatility, (low) level of invasiveness, and acquisition of different anatomical structures such as soft and bony tissues. The anisotropy of volumetric medical data is commonly solved by applying shape-based interpolation techniques [RU90] through the insertion of intermediate slices. To improve the data resolution and reduce morphological artifacts, we present local approximation methods that conjugate different features, such as approximation accuracy and extrapolation capabilities higher than linear precision methods; robustness with respect to data discretization; computational efficiency. These techniques are also useful for the generation of volume meshes for biomechanical simulations in orthopedics. Then, raw medical images are converted into volumetric data and a surface mesh is generated through the Marching Cube algorithm [ACMS97, LC87, KBSS01], level-sets methods [Whi00], and elastic surface nets [Gib98, BVP$^+$00]. Finally, high resolution meshes are generated and decimated using quadratic error metrics [GH97] and progressive meshes [Hop96], thus removing local noise and artifacts within a given error.

After this processing, the data is manually segmented into target structures of soft and bony tissues through a generally time-consuming procedure, which requires a deep knowledge of the human anatomy and medical imaging. Assuming that the input data is a 3D surface model of an anatomical structure, we discuss automatic and semi-automatic segmentation methods for identifying and delimitating elongated structures such as blood vessels, bones, and muscles. Our aim is to define a segmentation that captures the main features of a given medical data set, through the analysis of geometric properties of the shape that are invariant under rotation

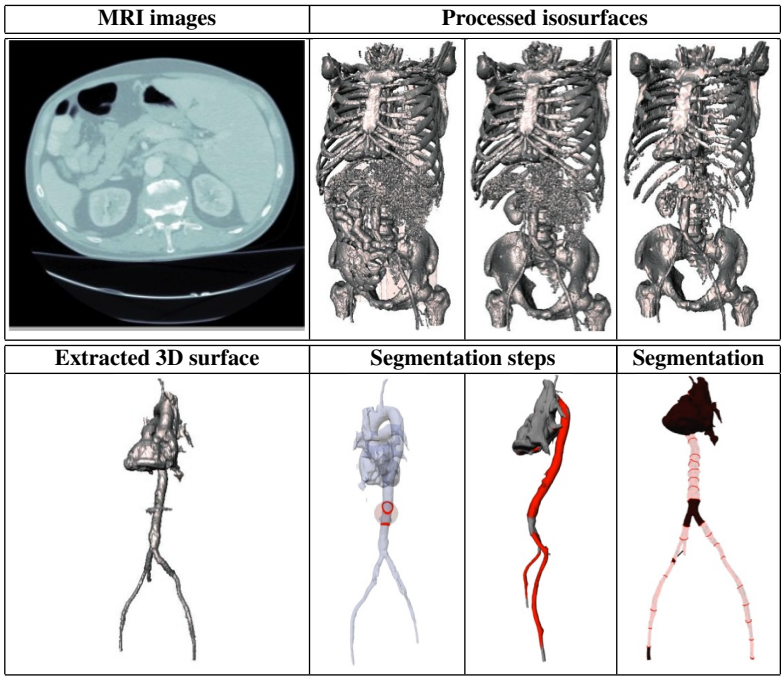

Fig. 1 Overall pipeline for modeling and analyzing medical data: input MRI images are converted into 3D models, which are smoothed, resampled, and simplified in order to remove geometric and topological artifacts. 3D meshes, which are manually identified, are then automatically segmented into tubular features (light red area), bodies and junctions (dark red regions).

and translation. Furthermore, we aim at distinguishing between global and local features, and organizing them into an abstract representation, which can be used to automate complex tasks such as shape comparison.

At the first stage of the proposed segmentation, muscles and organs are modeled with generalized geometrical primitives, such as tubular structures, bodies, and joints, also extracting anatomical relationships such as bone-muscles attachment sites. For each segmented part, geometric parameters (e.g., volume, area, curvature) that describe the morphology of the segments are extracted, thus providing a patient-specific information. These parameters, which cannot be extracted clinically, support a deeper and more accurate understanding of the underlying anatomy and pathologies, also allowing the discrimination between normal and problematic anatomical situations, as well as for a correct diagnosis. In fact, comparing segmented organs of a patient with reference models and parameters can be used to automatically identify possible abnormalities and to suggest a further analysis of the identified region. Furthermore, the extracted information is commonly used for planning surgical interventions, which require a precise localization of specific anatomical structures (e.g., tumors, vessels). For instance, the segmentation of articulations is difficult due to the proximity and overlap of different types of structures,

such as bones, muscles, and vessels, which generally have undefined boundaries. These boundaries also appear unclear in case of local degenerative pathologies such as osteoartrosis, cartilage degeneration, and calcifications.

The proposed multi-scale segmentation into main bodies (e.g., heart, muscles) and limb features (e.g., vessels) allows the construction of structural representations of the input data. These decompositions and the corresponding skeletal representations naturally follow the shape and extent of the limb features. Furthermore, the extracted skeletons are particularly useful for supporting further inspections through camera navigation and virtual surgery. Among the several skeletal representations of volumetric and surface data, we focus our attention on the Reeb graph [Ree46, SKK91]. In the context of medical imaging, the Reeb graph for the identification and removal of small tunnels of 3D models [WHDS04], which are commonly introduced by iso-surfacing algorithms, surface encoding for efficient data transmission [LV99, SKK91, TSK97], and shape similarity [BMM$^+$03, BMSF06, HSKK01].

The segmentation into anatomical features and the extraction of morphological parameters are necessary to connect acquired data to their semantics. The knowledge underlying a specific aspect (e.g., morphology, disease, etc) of the physiological human can be extracted and organized into a global ontological framework with the final aim of capturing the complementary information. In this way, a systematic diagnosis of patient individual pathologies, enriched with semantics and the development of ontologies in specific contexts (e.g., muscoloskeletal diseases of the hip, knee, femur, etc), support the clinician in all the phases of his/her activities. Connecting the analysis of medical data with their underlying semantics allows an individual monitoring of specific diseases for an objective quantification of the medical/surgical treatment and its follow-up. Finally, it is possible to query the 3D model for semantic information and integrate the semantic descriptors into the model itself, as well as the modeling and simulation processes.

In our preliminary study, the ontology codes information related to the setting for magnetic resonance imaging. Among them, we mention parameters related to the sagittal, axial, and coronal view; scan options such as fat suppression, availability of partial data, magnetic transfer; slice parameters, which include the numbers of slices, the slice size, and the acquisition range. Focusing on the knee district, the ontology includes five main classes; i.e., (i) femur, (ii) tibia, (iii) cartilage, (iv) ligaments, (v) meniscus. Then, the following terms can be used to annotate the cartilage, ligament, and meniscus: (i) femoral, tibial cartilage; (ii) medial, lateral, collateral ligament; (iii) anterior, posterior cruciate; (iv) medial, lateral meniscus. Fig. 1 shows the overall pipeline for modeling and analyzing medical data with computational methods.

The paper is organized as follows. We introduce local approximation techniques for modeling (Sect. 2), segmenting (Sect. 3), and abstracting (Sect. 4) medical data. Then, we discuss how the knowledge underlying medical data can be extracted (Sect. 5). Finally, we discuss open issues and future work (Sect. 6).

2 Local approximation techniques for modeling medical data

The anisotropy of volumetric medical data is commonly solved by applying shape-based interpolation techniques [RU90] through the insertion of intermediate slices. Alternatively, global approximation schemes [DLR86, Mic86, Wen95, MKB$^+$08, TO02] and the multi-level Partition of the Unity (PU) [OBA$^+$03] apply interpolating or least-squares (LS) constraints *globally*; then, the resulting approximation is evaluated at any sample point. Since MLS approximations [DLR86, Mic86, Wen95] and the multi-level Partition of the Unity [OBA$^+$03] involve a polynomial basis, they cannot be used to apply interpolating constraints in a simple way. In fact, the degree of the fitting polynomial determines the number of interpolating conditions and not *viceversa*. For instance, in 3D a polynomial of degree two or three requires to impose ten or nineteen interpolating constraints; however, we might have a different number of points in different neighbors. Furthermore, in case of uneven sampling fixing the number of points in each neighbor instead of its radius, or increasing the polynomial degree, provides unstable results due to the ill-conditioning of the corresponding Gram matrices [GV89]. After the data approximation, raw medical images are converted into volumetric data and a surface mesh is generated through the Marching Cube algorithm [ACMS97, LC87, KBSS01], level-sets methods [Whi00], and elastic surface nets [Gib98, BVP$^+$00].

To improve the data resolution and reduce morphological artifacts, in the following we present local approximation methods [PS12] that conjugate different features, such as approximation accuracy and extrapolation capabilities higher than linear precision methods; robustness with respect to data discretization; computational efficiency. Using a set of radial instead of polynomial basis functions, the proposed approach allows us to combine interpolating constraints for feature preservation and LS conditions for noise removal. In fact, the number of local interpolating constraints is equal to the number of RBFs and no more related to the degree of the polynomial used for the local approximation. In this way, we improve the flexibility in the design of scalar functions with sparse constraints [JGR09], which uses the PU and reproduces only linear maps.

In the following, we address the computation of the map $F : \mathbb{R}^d \to \mathbb{R}$ underlying a discrete scalar function $f : \mathscr{P} \to \mathbb{R}$, defined on a set $\mathscr{P} := \{\mathbf{x}_i\}_{i=1}^n$ of points in $\mathbb{R}^d$, which have been sampled on a 2D image ($d := 2$), a surface or a volumetric domain ($d := 3$). For 2D and 3D images the values of $f : \mathscr{P} \subseteq \mathbb{R}^d \to \mathbb{R}$, $d := 2,3$, are the pixels' intensity, the set $\mathscr{P}$ is the pixel grid, and the new sampling grid $\mathscr{S}$ is finer or coarser than $\mathscr{P}$ in case of up- or down-sampling, respectively. Due to the regularity of the 2D image grid, $\mathscr{N}_{\mathbf{x}}$, $\overline{\mathscr{N}_{\mathbf{x}}}$ are the 4- and 8-connected neighbors of $\mathbf{x}$. For 3D images, the neighbors are defined in a similar way.

The map $F : \mathbb{R}^d \to \mathbb{R}$ underlying $f : \mathscr{P} \to \mathbb{R}$ is defined as a function that *locally* interpolates or approximates the f-values. The idea behind the proposed approach is to compute $F(\mathbf{x})$, $\mathbf{x} \in \mathbb{R}^d$, by imposing the f-values at the points of a neighbor $\mathscr{N}_{\mathbf{x}}$ of $\mathbf{x}$ as interpolating or least-squares constraints. This choice is motivated by the observation that the behavior of any approximation of f at $\mathbf{x}$ is mainly controlled by the f-values in $\mathscr{N}_{\mathbf{x}}$. Indeed, the evaluation point $\mathbf{x}$ drives the selection of a set of

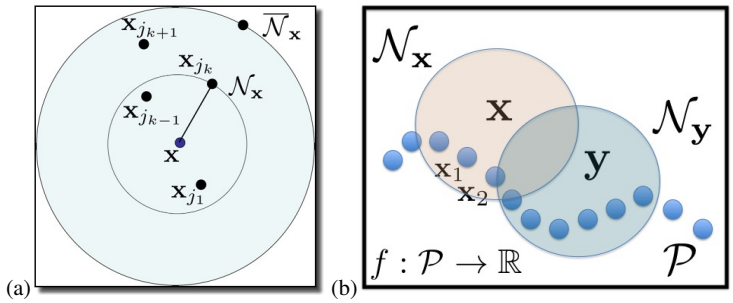

Fig. 2 (a,b) Neighbors $\mathscr{N}_{\mathbf{x}}$ and $\overline{\mathscr{N}}_{\mathbf{x}}$ of $\mathbf{x}$, $\mathscr{N}_{\mathbf{x}} \subseteq \overline{\mathscr{N}}_{\mathbf{x}}$, used for the computation of the value $F(\mathbf{x})$.

interpolating conditions and the construction of the local approximation F in $\mathscr{N}_{\mathbf{x}}$. On the contrary, previous work applies these constraints *globally*; i.e., the function $F : \mathbb{R}^d \to \mathbb{R}$ that satisfies *all* the interpolating conditions $F(\mathbf{x}_i) = f(\mathbf{x}_i)$, $i = 1, \ldots, n$, is computed and then F is evaluated at any point $\mathbf{x}$.

Local approximation with interpolating constraints

Firstly, we compute the function $F : \mathbb{R}^d \to \mathbb{R}$ that interpolates the values of f at the points of $\mathscr{N}_{\mathbf{x}}$; i.e., $F(\mathbf{x}_{j_s}) = f(\mathbf{x}_{j_s})$, $s = 1, \ldots, k$. Here, the neighbor $\mathscr{N}_{\mathbf{x}} := \{\mathbf{x}_{j_s}\}_{s=1}^{k}$ includes those points of $\mathscr{P}$ that fall inside the sphere of center $\mathbf{x}$ and radius $\sigma(\mathbf{x})$, which is chosen according to the local sampling density of $\mathscr{P}$ [PKKG03] (Fig. 2(a)). To this end, we consider the map $F : \mathbb{R}^d \to \mathbb{R}$, which is the linear combination of the RBFs $\mathscr{B} := \{\phi_{j_s}(\mathbf{x}) := \phi(\|\mathbf{x} - \mathbf{x}_{j_s}\|_2)\}_{s=1}^{k}$; i.e.,

$$\begin{cases} F(\mathbf{x}) := \sum_{s=1}^{k} \beta_s(\mathbf{x}) \phi_{j_s}(\mathbf{x}) = \beta^T(\mathbf{x}) \tilde{\phi}(\mathbf{x}), \\ \beta(\mathbf{x}) := (\beta_s(\mathbf{x}))_{s=1}^{k}, \quad \tilde{\phi}(\mathbf{x}) := (\phi_{j_s}(\mathbf{x}))_{s=1}^{k}. \end{cases} \tag{1}$$

Each function ϕ_{j_s} is generated by a map $\phi : \mathbb{R}^+ \to \mathbb{R}$ and centered at $\mathbf{x}_{j_s}$ [DLR86, Mic86]. We also assume that the corresponding kernel $K(\mathbf{x}, \mathbf{y}) := \phi(\|\mathbf{x} - \mathbf{y}\|_2^2)$, $\mathbf{x}, \mathbf{y} \in \mathbb{R}^d$, is positive definite; i.e., the Gram matrix associated to $K(\cdot, \cdot)$ is positive definite. Imposing these interpolating conditions, the coefficient vector $\beta(\mathbf{x})$ in Eq. (1) solves the linear system $\Phi\beta(\mathbf{x}) = \mathbf{f}_k$, $\Phi := (\phi_{rs})_{r,s=1}^{k}$, where Φ is the $k \times k$ Gram matrix associated to the generating map ϕ with respect to the points of $\mathscr{N}_{\mathbf{x}}$, whose entries are $\phi_{rs} := \phi(\|\mathbf{x}_{j_r} - \mathbf{x}_{j_s}\|_2)$, and $\mathbf{f}_k := (f(\mathbf{x}_{j_s}))_{s=1}^{k}$ is the $k \times 1$ array of the corresponding function values.

Local approximation with least-squares constraints

Interpolating the f-values allows us to precisely reproduce the local behavior of f but is error-prone in case of noisy data. To overcome this drawback, we re-

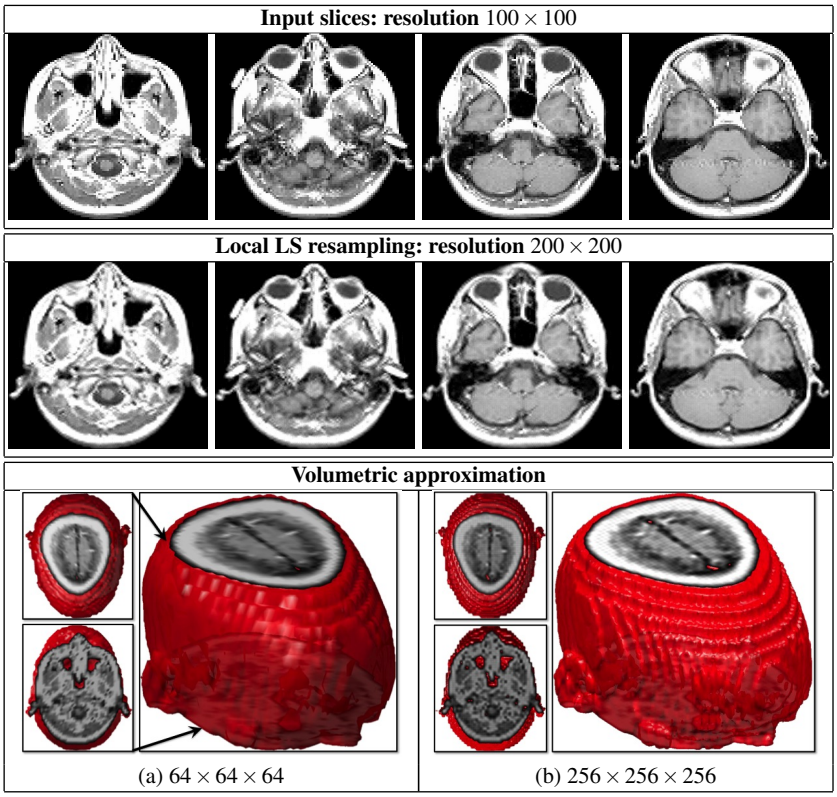

Fig. 3 (Second row) Local LS approximation of (first row) a low-resolution and noisy medical data set. Iso-surfaces related to the (a) input and (b) resampled data set.

place interpolating with LS constraints (Fig. 2(b)). Recalling that in $\mathscr{N}_{\mathbf{x}}$ the function $F : \mathbb{R}^d \to \mathbb{R}$ underlying $f : \mathscr{P} \to \mathbb{R}$ is a sum of RBFs centered at the points of $\mathscr{N}_{\mathbf{x}}$, the local LS approximation takes into account the f-values at the points of a neighbor $\overline{\mathscr{N}}_{\mathbf{x}}$ larger than $\mathscr{N}_{\mathbf{x}}$. In our tests, $\overline{\mathscr{N}}_{\mathbf{x}}$ is the neighbor of $\mathbf{x}$ whose radius is twice the radius of $\mathscr{N}_{\mathbf{x}}$. Then, F is computed by minimizing the error $\sum_{s=1}^{h} |F(\mathbf{x}_{j_s}) - f(\mathbf{x}_{j_s})|^2$ through the normal equation

$$(\boldsymbol{\Phi}^T \boldsymbol{\Phi})\beta(\mathbf{x}) = \boldsymbol{\Phi}^T \mathbf{f}_h, \quad \boldsymbol{\Phi} := (\phi_{sr})_{s=1,\ldots,h}^{r=1,\ldots,k}, \tag{2}$$

where $\phi_{sr} := \phi(\|\mathbf{x}_{j_r} - \mathbf{x}_{j_s}\|_2)^2$, $\overline{\mathscr{N}}_{\mathbf{x}} := \{\mathbf{x}_{j_s}\}_{s=1}^{h}$, $k \le h \le n$, and $\mathbf{f}_h := (f(\mathbf{x}_{j_s}))_{s=1}^{h}$ is the $h \times 1$ right-hand side vector. Since $\boldsymbol{\Phi}$ is a full-rank matrix, $(\boldsymbol{\Phi}^T \boldsymbol{\Phi})$ is invertible and Eq. (2) has a unique solution. If $\mathscr{N}_{\mathbf{x}} = \overline{\mathscr{N}}_{\mathbf{x}}$, then the local approximations with interpolating and LS constraints are the same.

In Fig. 3, the local approximation with LS constraints of 2D images have been resampled at a higher resolution. Complex features, which are located where different tissues and bones touch each others, are accurately approximated. In Fig. 4, the

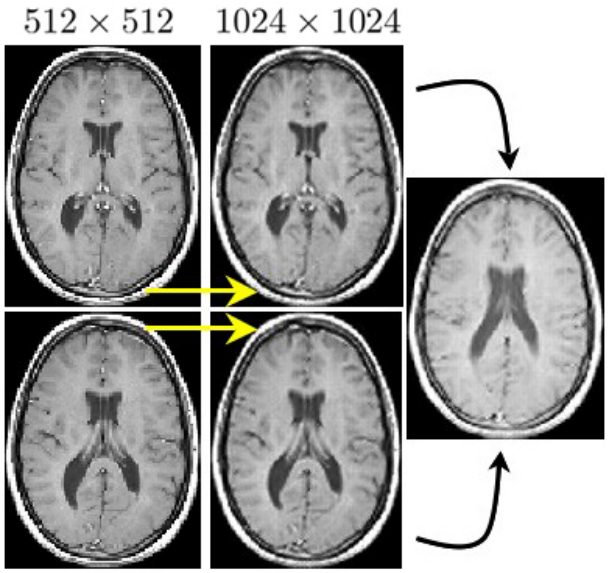

Fig. 4 The input images (first column) have been approximated with the implicit LS approximation (second column) at a double resolution. Then, the resulting approximation has been sampled on a new slice in-between the input ones (right picture).

local approximation with RBFs of medical data acquired on two consecutive slices of a human head has been resampled on an intermediate slice without performing a new acquisition, which is generally time-consuming and possibly intractable (e.g., nocivity, health problems, etc.). Since the number of points in each neighbor is generally small (e.g., $20 \leq k \leq 30$), we consider a generating map ϕ with a global support. Common choices of ϕ are the Gaussian $\phi(t) := \exp(-t/\sigma)$ and the bi-harmonic $\phi(t) := |t^3|/\sigma$ kernel, where the support σ is computed according to [DS05, MN03] and adapted to the local sampling of $\mathscr{P}$.

Computational cost

Since a $n \times n$ linear system is solved once, the computational cost of the approximation with globally- and locally-supported radial basis functions (RBFs) is $O(n^3)$ and $O(n \log n)$, respectively. In the proposed approach, we solve a linear system once for each sample point and the evaluation of the resulting approximation at s points takes $O(sk^3)$ time. Indeed, its computational cost is generally lower than the approximation with globally- and locally-supported RBFs. It also reduces the memory storage from $O(n^3)$ and $O(kn)$ to $O(k^3)$. Finally, our method has the same order of complexity of local approximation schemes, such as the moving least-squares approximation [DLR86, Mic86, Wen95] and the multi-level Partition of the Unity [OBA$^+$03].

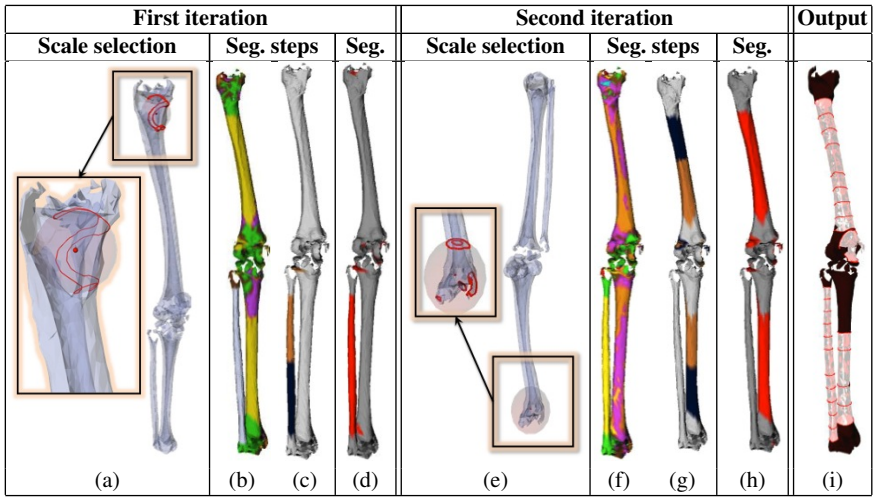

Fig. 5 Multi-scale identification of tubular features at two (a-d,e-h) different scales and (i) final segmentation.

3 Segmentation and morphological analysis of medical data

Shape segmentation is achieved by constructing a computational description of shape features, usually a few basic types, possibly along with their relationships. For medical data, the complexity of the understanding process increases due to the lack of formal definitions of shape features. The paradigm of shape segmentation, analysis, and abstraction is strongly influenced by the targeted application context. In general, we observe that an ideal shape segmentation of medical data should be able to capture and compute the main features of the input data and should be based on geometric properties of the shape that are invariant under rotation and translation. Furthermore, it should distinguish between global and local features, and organize them into an abstract representation which can be used to automate complex tasks such as shape comparison. In fact, comparing segmented organs of a patient with reference models and parameters can be used to automatically identify possible abnormalities and to suggest a further analysis of the identified region.

Assuming that the input data is a 3D surface model of an anatomical structure, we now discuss automatic and semi-automatic segmentation methods for identifying and delimitating elongated structures such as blood vessels and muscles. In the context of the segmentation of 3D shapes extracted from medical data, the method described in [MPS$^+$04a, MPS$^+$04b] defines a shape decomposition into connected components that are either *tubular features*, identified by regions that can be described as generalized cones or cylinders (e.g., handle-like and protrusion-like features, together with their concave counterparts), and *body regions* identified by patches which connect tubular features. The shape segmentation works in a multi-scale setting (i.e., using a fine-to-coarse strategy), starting with the extraction of

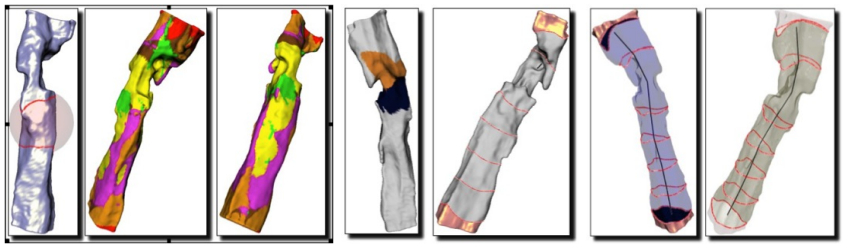

(a) (b) (c)

Fig. 6 (a) Morphological shape analysis, (b) identification of the tubular features, and (c) its graph.

small tubes first; during the iterative procedure, triangles are marked as visited and are not taken into account at the following steps. These scales are automatically set by uniformly sampling the interval between the minimum edge length and the diagonal of the bounding box of the input shape; however, the user can tune the levels of detail if he/she has some *a-priori* information or if he/she is searching for features of specific dimension. Furthermore, the multi-scale approach reduces the influence of noise on the shape evaluation, ensures a greater flexibility to formulate filters for shape analysis, and captures the more representative properties in a detailed description. At the end of the whole process, tubes are labeled as generalized cones or cylinders and are associated to the scale at which they have been found. Each conical or cylindrical (tubular) feature, extracted at a given scale, is abstracted by a skeletal line together with morphological features.

For each segmented part, parameters that describe the morphology of the segments are extracted, thus providing a patient-specific segmentation. We also notice that all these measurements cannot be performed clinically and can be used to assist the analysis of morphological abnormalities of tubular structures. For instance, this segmentation also represents the first step toward the identification of tissue components, which are likely to have mechanical interactions in-between, contact between bones and tissues in-between articulating surfaces and ligaments. This segmentation supports the identification or relocation of feature points, which are commonly used for simulation purposes. For the knee district, the coordinates of the medial/lateral femoral condyle, proximal/distal femur, and proximal tibia can be improved through the segmentation of the anatomical regions extracted by the proposed approach.

In Fig. 5, we consider the multi-scale segmentation of a 3D shape representing the leg bones. At the first scale (a), we select the radius of the sphere gives the size of the features that will be identified through (b) a multi-scale curvature analysis and (c) the identification of the medial loops of the tubular feature, which is identified by sweeping the medical loop on the input shape (d). Then (e-h), we select a larger scale and run the same process until (i) the all the tubular features and joints have been identified. Features previously identified are no more visited. Examples of segmentations and skeletons of anatomical structures are shown in Figs. 6, 7.

The surface decomposition, the skeletal lines of tubular features, and their spatial arrangement defines a *shape-graph*, whose nodes are the extracted primitive shapes,

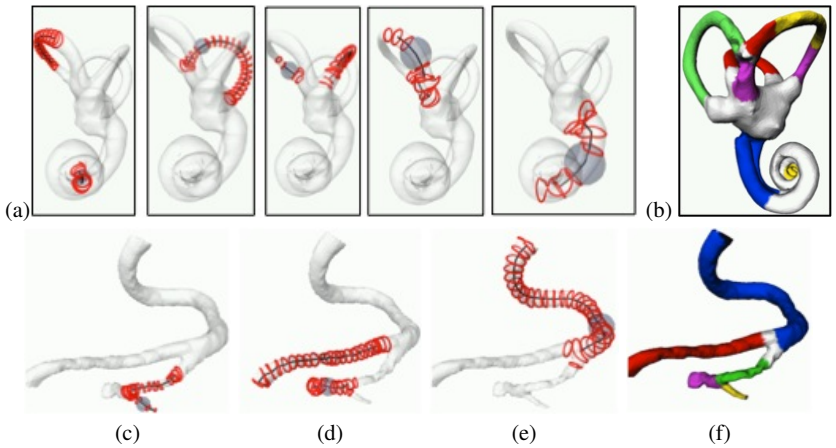

Fig. 7 Level-sets and skeleton of tubular features of a (a) cochlea and (c-e) vessel; (b,f) corresponding segmentations into tubular features. Different colors identify features at different scales.

while the arcs code the adjacency relationships among them. Finally, each arc is classified as handles or junctions depending on the mutual position between each tubular feature and adjacent regions which can be bodies or tubes. Approximating each tube with truncated cones of circular bases, each having the same length of the corresponding tube cross section, enables to calculate an approximation of the feature volume. The extracted shape graph is particularly useful for supporting further inspections through camera navigation and virtual surgery. Finally, the segmentation into anatomical features and the extraction of morphological parameters are necessary to connect acquires data to their semantics (Sect. 4).

4 Abstraction of medical data

A skeletal representation yields a compact and expressive shape abstraction, which attempts to reflect the human intuition. The use of sufficiently concise, informative, and easily computable skeletal representations, instead of the whole models, may facilitate the comparison process. In fact, the search in a database for an object similar to a query can be nearly impossible if approached by simply comparing point clouds or bulks of thousand triangles. A way to bypass the aforementioned problems is to code the input shape as a skeleton representation. Important aspects that drive the definition of a skeletal representation are the invariance to translations, rotations, and scalings; the identification and abstraction of shape features; the independence of the representation with respect to the shape embedding and discretization; the property of being medial with respect to the shape.

The definition of skeletal representations is approached by: (i) defining a *medial* structure representation that always falls inside the shape and is equidistant

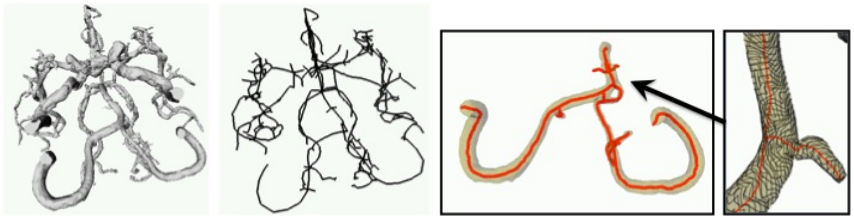

(a) (b) (c)

Fig. 8 (a) Input 3D model of a vessel, (b) its Reeb graph, and (c) zoom-in.

from the shape boundary at each point or (ii) explicitly representing how the basic components of the shape are glued together to form the whole. Main examples of medial representations are: the Medial Axis [Blu67, BSTZ07, SP07], which in 3D may contain both curve segments and sheets with non-manifold connections; the medial curves computed through segmentation [CAL$^+$04, CDS$^+$05, KT03]; the medial geodesic skeleton [DS06]; the mesh contraction based on Laplacian smoothing [ATC$^+$08] and surface-based operations [AAAG95, CSYB05, SNdB02]. Among several skeletal representations, in the following we focus our attention on the Reeb graph. In the context of medical imaging, the Reeb graph is useful to identify and remove small tunnels of 3D models [WHDS04], which are commonly introduced by iso-surfacing algorithms. Additional applications include surface deformations [LCF00, WSLG07, YHMY08, YBS07], surface encoding for efficient data transmission [LV99, SKK91, TSK97], and shape similarity [BMM$^+$03, BMSF06, HSKK01].

Differential topology [BFD$^+$] provides a suitable framework for formalizing and solving several problems related to shape understanding due to the theoretical link between critical points, their configuration, and the topological properties of the input surface. Given a scalar function $f : \mathscr{M} \to \mathbb{R}$, defined on a manifold surface $\mathscr{M}$, the topology of $\mathscr{M}$ can be effectively studied by contracting the connected components of the level-sets $\gamma_\alpha := \{\mathbf{p} \in \mathscr{M} : f(\mathbf{p}) = \alpha\}$ of f to single points (i.e., the *Reeb graph*) or joining its critical points (i.e., $\{\mathbf{p} \in \mathscr{M} : \nabla f(\mathbf{p}) = \mathbf{0}\}$) with flow-lines of f (i.e., the Morse-Smale complex). The Reeb graph and the Morse-Smale complex provide an abstract representation of the surface $\mathscr{M}$. The former is based on the topological changes of the level-sets of f, the latter mainly uses the connectivity of the critical points with respect to the behavior of the gradient field of f. The most interesting aspect of this approach is its parametric nature: changing f we have different descriptions of the same surface $\mathscr{M}$ which highlight different "local" features while preserving the "global" topological structure of $\mathscr{M}$. Indeed, the *Reeb graph* [Ree46] codes the evolution and arrangement of the level sets of a real function $f : \mathscr{M} \to \mathbb{R}$, defined over a manifold $\mathscr{M}$. The Reeb graph is always a 1-dimensional complex and in its original definition provides a description that is not invertible. This means that the input shape cannot be exactly recovered from the Reeb graph and the geometric information stored in its nodes and arcs. Changing the scalar function allows us to tackle the resulting Reeb graph to shape

comparison [HSKK01], segmentation [BBP09], and visualization [TGSP09]. Examples of functions effectively used in applications are geodesic distances, harmonic and Laplacian eigenfunctions. Efficient algorithms for the computation of the Reeb graph exist for polyhedral surfaces [CMEH$^+$03, PSF09], volume models [TGSP09], and higher dimensional data [PSBM07, DN09, HWW10].

For the computation of the Reeb graph, sweeping techniques [CSA03, CLLR05, CMEH$^+$04, LV99, PCMS04, PSBM07] and sampling-based approaches [SKK91] have been proposed. The idea behind the minimal contouring algorithm [PSF08] for the computation of the Reeb graph is to study the evolution of the level-sets only at saddle points without sampling or sweeping the image of f. Instead of building an injective correspondence between the vertices of $\mathscr{M}$ and the nodes of the Reeb graph, our algorithm stores only a minimal information on the behavior of f on $\mathscr{M}$. In fact, each node of the computed Reeb graph is associated either with a critical point of f (i.e., maximum, minimum, saddle point) or with one of the level-set passing through a saddle point. Each arc of the Reeb graph is associated with a region $\mathscr{S}$ of $\mathscr{M}$ that is delimited by the critical loops; in $\mathscr{S}$, all the iso-contours are related to regular iso-values of f and are homeomorphic. The family of these regions provides a hierarchical shape segmentation into 0-genus patches, which are classified as generalized cones, cylinders, pants, and characterized through morphological parameters such as areas and volumes. Examples of skeletons of vessels are shown in Figs. 6(c), 8(b,c).

5 Semantic analysis of medical data

While the technological advances in terms of hardware and software have made available plenty of tools for visualizing medical data and interacting with their geometry, the interaction with the underlying semantics is still far from being satisfactory. It is rather difficult to search 3D data by their semantic meaning, which describes a pathology, a specific stadium or configuration of the pathology itself. This is partly due to the lack of methods for the automatic extraction of the semantic content (*semantic annotation*) and to the evolution of research on data modeling, which had to be highly focused on the visual and geometric aspects of the data.

From geometry to semantic annotation of medical data

The shift from a purely geometric to a semantic-aware level of representation of medical data requires tools that generate effective high-level computational models that describe shapes and their structures through the analysis of the information available (geometry, topology, application context, ...). Recent research is focused on the extraction of semantic information based on a decomposition of the input shape into building primitives, whose meaning is defined by the underlining application context. The approach to modeling medical data, which represents organs,

tissues, bones, and their semantics is based on the assumption that what is common to all shapes is that they have a geometry, they can be described by structures (object features and part-whole decomposition), they have attributes (morphological parameters, anatomical names, attached to an object, its parts and/or its features), they have a semantics (meaning, purpose), and they may also have interaction with time (e.g., acquisition history, temporal series, FEM simulation). Furthermore, the rapid evolution of semantic-based knowledge systems and the definition of medical ontologies [htt03] is opening new possibilities for an intelligent exploitation of medical data. In fact, metadata and ontologies can be used to support and store the analysis and understanding of acquired medical data.

Knowledge formalization is useful to manage structural, functional, and topological information extracted from the medical data, and couple them with expertise and know-how of the physicians. Knowledge plays a role for anatomy as well as physiological and pathological parameters in health applications. As main examples in medicine, we can consider the simulation of the replacement of articulation prosthesis. From a medical perspective, the main steps include bone resection, prosthesis alignment, and checking of motion amplitudes. From the knowledge-based perspective, the parameters of interest are contact pressure within the cartilages. Another example scenario is the virtual anatomy, i.e., the elaboration of 3D geometry models of human anatomy. The use of knowledge-based techniques has also benefits on patient specific computer assisted therapy planning; here, the term assisted therapy refers to all the steps in-between the planning of the surgery operation, the re-habilitation, and the eventual follow-up. According to the medical paradigms, it is common to distinguish between generic anatomy atlases, which demonstrate anatomical structures and their relationships, and individual anatomy. The latter is of special interest when pathological situations need further attention with respect to a medical treatment. Generic anatomy models are carefully designed using modeling software, whereas patient specific anatomy models come as output of a scanning device, associated with point set based or image-based reconstruction algorithms.

The objective of ontology building is to identify the terminology, key concepts, and properties of complex data, and key relationships describing various phases of interaction and processing with the data. This goal requires the conceptualization of the domain of application. The ontology design of 3D data, and more generally 3D media [VGRP$^+$10], is critical because its output is the first concrete sketch of ontology structure. This step identifies the domain of the ontology, the relevant usage scenarios, the knowledge sources (domain experts, glossaries and dictionaries, etc.), and the basic questions that the ontology should be able to answer. These basic questions are called Competency Questions (CQs) and essentially constitute expressiveness requirements for the ontology. In medicine, taxonomies are used for particular needs (e.g., medical record, health insurance, clinical billing), but they do not really deal with the geometric representation of organs, tissues, or other relevant 3D measures. An example of segmentation and semantic annotation of the knee district, which can be refined by combining more sophisticated shape segmentation techniques and a richer class of terms, is shown in Fig.9(a).

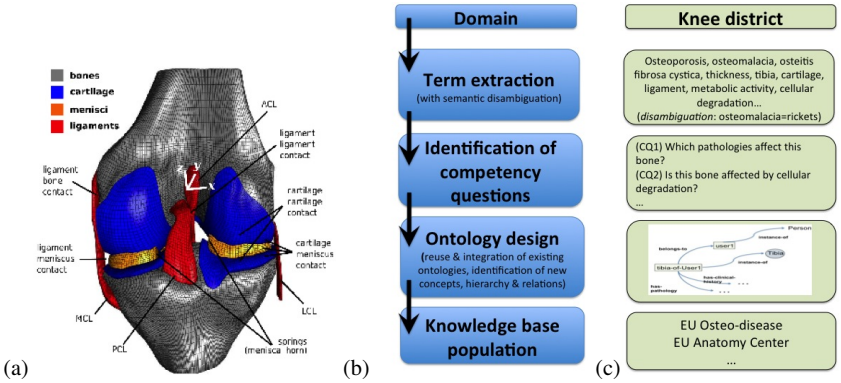

Fig. 9 (a) Geometric model of the knee and its semantic annotation, which can be refined by combining more sophisticated shape segmentation techniques and a richer class of terms. (b) Ontology conceptualization and (c) its application to the knee district. The terms of the ontology can also be linked to segmented patches through semantic annotation.

Ontologies in medical applications

A key element in the development of intelligent platforms for healthcare is the integration of quantitative parameters extracted from multi-modality imaging techniques, with the final aim of generating more accurate predictive models of normal and dysfunctional behavior. In this way, a systematic diagnosis of patient individual pathologies will support the clinician in all the phases of his/her activities. To achieve these goals, a key concept is the development of an ontology that allows the harmonization of the concepts related to the physiological human into a knowledge-driven framework able to provide access and links to data and concepts properly described via a shared conceptualization.

As the NCBI Taxonomy browser [BKML$^+$09, WBB$^+$08] shows, the field is very active. In the eighties, the efforts made by the US National Library of Medicine lead to the first ontologies to help access to publication and online data. These first developments lead to MeSH2, UMLSR3 and the NCI thesaurus. With the development of genomics and proteomics, the amount of experimental data has increased very fast in the last twenty years and the need for terminologies has been driving bioinformatics research. In the late nineties, the *Gene Ontology* (GO), the *Encyclopedia of Escherichia coli K-12 Genes and Metabolism* (EcoCyc), the *Ontology for Molecular Biology and Bioinformatics* (MBO), the *Transparent Access to Multiple Bioinformatics Information Sources* (TAMBIS), and the *RiboWeb* appeared, leading the way to ontologies for bioinformatics. Ontology development is also a major field in bioinformatics [SWLG03]. Bioinformatics shares ontologies with biomedicine and some of the ontologies are used in various fields in biology. It is important to mention the recent initiative of the W3C on *Linking Open Drug Data* (LODD) [htt], which is related to information about drugs that is available on the Web. The sources of data range from impacts of the drugs on gene expression, through to the results

of clinical trials. The LODD project focuses on linking the various sources of drug data together to answer interesting scientific and business questions. The linking data paradigm seems particularly useful for modeling the knowledge underlying osteo-diseases as it may allow the seamless correlation of ontology-based descriptions of items belonging to different ontological descriptions.

Development of novel ontologies in medical applications

Although many ontologies for biological and healthcare data exists there has been little progress made on ontologies that attempt to capture the complementary information and accessibility required for multi-modal and multi-scale data. The most suitable methodology will be adopted to create a network of cross-references among existing and valuable ontologies, possibly complemented with new ones, in order to provide a global view of the knowledge pertaining to a specific domain. To achieve the aforementioned goals, the Linking Open Data initiative seems the most promising methodology. Finally, the knowledge underlying the physiological human will be extracted and organized into a global ontological framework with the final aim of capturing the complementary information and accessibility required for multi-modal and multi-scale data.

An intelligent platform for healthcare requires visualization and analysis tools, together with a formalization of the underlying medical knowledge. Indeed, domain ontologies have been developed for analyzing and sharing patient data and medical concepts related to a specific pathology. This formalization must satisfy different needs, such as the use of a medical terminology, the definition of concepts with a unique and non-ambiguous meaning, the consensus of the medical community, the conceptualization of a wide range of concepts and their relations. The first step is the identification of the terminology, key concepts, and properties of the different phases of the physiological human that require a conceptualization (Fig. 9(a,b)). Indeed, the first step is to identify the domain of the ontology, relevant usage scenarios, knowledge sources (domain experts, glossaries, and dictionaries, etc.), and the basic questions (based on CQ concept) that the ontology should be able to answer. Usage scenarios, requirements specifications and competency questions will be used as reference for the evaluation. Particular attention will be devoted to the conceptualization of clinical cases, in order to provide a rich documentation of the experiences made by the surgeons when using the ontology. Let us briefly summarize the main steps for the construction of an ontology, with a specific focus on the medical scenario. An ontology includes*classes*, which are the concepts related to a specific domain; *relations*, which are binary relations between concepts; *instances*, which are single terms, commonly used in a specific domain.

Among the main features of an ontology-based platform, we mention: *basic browsing functionalities* (text and keyword search); *ontology visualization services*; *semantic search capabilities*, which will exploit reasoning on the underlying ontology; *classification services*, which will present pre-existing clinical cases grouped according to different criteria; *annotation services*, which allow the sur-

geons to attach any relevant information to the clinical cases. In our preliminary study (Fig. 9(c)), the ontology codes information related to the setting for magnetic resonance imaging. Among them, we mention parameters related to the sagittal, axial, and coronal view; scan options such as fat suppression, availability of partial data, magnetic transfer; slice parameters, which include the numbers of slices, the size tickles, and the acquisition range. Focusing on the knee district, segmented regions can be annotated with a first set of terms, which include five main classes; i.e., (i) femur, (ii) tibia, (iii) cartilage, (iv) ligaments, (v) meniscus. This process is semi-automatic and this annotation can be further specialized if spatial relations about the mutual position of the segments is available. More precisely, the following terms can be used to annotate the cartilage, ligament, and meniscus: (i) femoral, tibial cartilage; (ii) medial, lateral, collateral ligament; (iii) anterior, posterior cruciate; (iv) medial, lateral meniscus.

6 Conclusions and future work

This paper has reviewed and discussed a number of computational methods for modeling and analyzing the morphology of anatomical structures, their spatial features and relations, together with their abstraction and the extraction of the underlying semantics. Integrating computational methods developed in Computer Graphics, knowledge base, and simulation will allow the generation of more accurate predictive models of normal and dysfunctional behavior. In this way, a systematic diagnosis of patient individual pathologies will support the clinician in all the phases of his/her activities. As future work, we plan to design and implement the ontology of the knee district and study the integration of segmentation methods with semantics.

Acknowledgements This work has been partially supported by the FP7 Marie Curie Initial Training Network *MultiScaleHuman*. Fig. 9(a) is courtesy of the OpenKnee Consortium.

References

[AAAG95] O. Aichholzer, D. Alberts, F. Aurenhammer, and B. Gartner. A novel type of skeleton for polygons. *Journal of Universal Computer Science*, 1:752–761, 1995.

[ACMS97] F. Allamandri, P. Cignoni, C. Montani, and R. Scopigno. Adaptively adjusting marching cubes output to fit a trilinear reconstruction filter. In *Proc. of Eurographics Workshop in Visualization*, 1997.

[ATC+08] O. K.-C. Au, C.-L. Tai, H.-K. Chu, D. Cohen-Or, and T.-Y. Lee. Skeleton extraction by mesh contraction. In *ACM Siggraph*, pages 1–10, 2008.

[BBP09] S. Berretti, A. Del Bimbo, and P. Pala. 3D Mesh Decomposition using Reeb Graphs. *Image and Vision Computing*, 27(10):1540–1554, 2009.

[BFD+] S. Biasotti, B. Falcidieno, L. De Floriani, P. Frosini, D. Giorgi, C. Landi, L. Papaleo, and M. Spagnuolo. Describing shapes by geometric-topological properties of real functions. *ACM Computing Surveys*, 40(4).

[BKML+09] D. A. Benson, I. Karsch-Mizrachi, D. J. Lipman, J. Ostell, and E. W. Sayers. GenBank. *Nucleic acids research*, 37:D26–31, 2009.

[Blu67] H. Blum. A transformation for extracting new descriptors of shape. In *Models for the Perception of Speech and Visual Form*, pages 362–380. MIT Press, 1967.

[BMM+03] S. Biasotti, S. Marini, M. Mortara, G. Patanè, M. Spagnuolo, and B. Falcidieno. 3D shape matching through topological structures. In *Discrete Gemetry for Computer Imagery*, pages 194–203, 2003.

[BMSF06] S. Biasotti, S. Marini, M. Spagnuolo, and B. Falcidieno. Sub-part correspondence by structural descriptors of 3D shapes. *Computer-Aided Design*, 38(9):1002–1019, 2006.

[BSTZ07] S. Bouix, K. Siddiqi, A. Tannenbaum, and S. W. Zucker. *Statistics and Analysis of Shapes*. Springer, 2007.

[BVP+00] P. W. de Bruin, Frans Vos, Frits H. Post, Sarah F. Frisken Gibson, and Albert M. Vossepoel. Improving triangle mesh quality with surfacenets. In *Proc. of the International Conference on Medical Image Computing and Computer-Assisted Intervention*, pages 804–813, 2000.

[CAL+04] J.-H. Chuang, N. Ahuja, C.-C. Lin, C.-H. Tsai, and C.-H. Chen. A potential-based generalized cylinder representation. *Computers & Graphics*, 28(6):907 – 918, 2004.

[CDS+05] N. D. Cornea, M. F. Demirci, D. Silver, A. Shokoufandeh, S. J. Dickinson, and P. B. Kantor. 3D object retrieval using many-to-many matching of curve skeletons. In *Proc. of IEEE Shape Modeling and Applications*, pages 368–373, 2005.

[CLLR05] Y.-J. Chiang, T. Lenz, X. Lu, and G. Rote. Simple and optimal output-sensitive construction of contour trees using monotone paths. *Computational Geometry Theory and Applications*, 30(2):165–195, 2005.

[CMEH+03] K. Cole-McLaughlin, H. Edelsbrunner, J. Harer, V. Natarajan, and V. Pascucci. Loops in Reeb graphs of 2-manifolds. In *Proc. of the Symp. on Computational Geometry*, pages 344–350, 2003.

[CMEH+04] K. Cole-McLaughlin, H. Edelsbrunner, J. Harer, V. Natarajan, and V. Pascucci. Loops in Reeb graphs of 2-manifolds. *Discrete Computational Geometry*, 32(2):231–244, 2004.

[CSA03] H. Carr, J. Snoeyink, and U. Axen. Computing contour trees in all dimensions. *Computational Geometry Theory and Applications*, 24(2):75–94, 2003.

[CSYB05] N. D. Cornea, D. Silver, D. Yuan, and R. Balasubramanian. Computing hierarchical curve- skeletons of 3D objects. *The Visual Computer*, 21(11):945–955, 2005.

[DLR86] N. Dyn, D. Levin, and S. Rippa. Numerical procedures for surface fitting of scattered data by radial functions. *SIAM Journal on Scientific and Statistical Computing*, 7(2):639–659, 1986.

[DN09] H. Doraiswamy and V. Natarajan. Efficient algorithms for computing Reeb graphs. *Computational Geometry: Theory and Applications*, (42):606–616, 2009.

[DS05] T. K. Dey and J. Sun. An adaptive MLS surface for reconstruction with guarantees. In *ACM Symp. on Geometry Processing*, pages 43–52, 2005.

[DS06] T. K. Dey and J. Sun. Defining and computing curve-skeletons with medial geodesic function. In *Proc. of Symp. on Geometry Processing*, pages 143–152, 2006.

[GH97] M. Garland and P. S. Heckbert. Surface simplification using quadric error metrics. In *ACM Siggraph*, pages 209–216, 1997.

[Gib98] S. F. Gibson. Constrained elastic surface nets: Generating smooth surfaces from binary segmented data. In *Proc, of the International Conference on Medical Image Computing and Computer-Assisted Intervention*, pages 888–898, 1998.

[GV89] G. Golub and G.F. VanLoan. *Matrix Computations*. John Hopkins University Press, 2nd Edition, 1989.

[Hop96] H. Hoppe. Progressive meshes. In *ACM Siggraph*, pages 99–108, 1996.

[HSKK01] M. Hilaga, Y. Shinagawa, T. Kohmura, and T. L. Kunii. Topology matching for fully automatic similarity estimation of 3D shapes. In *ACM Siggraph*, pages 203–212, 2001.

[htt] http://esw.w3.org/topic/HCLSIG/LODD. Linking open drug data (LODD).

[htt03] http:www.nlm.nih.gov/research/umls. Unified medical language system, national library of medicine. *Technical Report*, 9, 2003.

[HWW10] W. Harvey, Y. Wang, and R. Wenger. A randomized $O(m \log m)$ time algorithm for computing Reeb graphs of arbitrary simplicial complexes. In *ACM Symp. on Computational Geometry*, 2010.

[JGR09] J. Jin, M. Garland, and E. A. Ramos. MLS-based scalar fields over triangle meshes and their application in mesh processing. In *Proc. of the Symp. on Interactive 3D Graphics and Games*, pages 145–153, 2009.

[KBSS01] L. Kobbelt, M. Botsch, U. Schwanecke, and H.-P. Seidel. Feature sensitive surface extraction from volume data. In *ACM Siggraph*, pages 57–66, 2001.

[KT03] S. Katz and A. Tal. Hierarchical mesh decomposition using fuzzy clustering and cuts. *ACM Siggraph*, pages 954–961, July 2003.

[LC87] W. E. Lorensen and H. E. Cline. Marching cubes: A high resolution 3D surface construction algorithm. *ACM Siggraph*, 21(4):163–169, 1987.

[LCF00] J. P. Lewis, Matt Cordner, and Nickson Fong. Pose space deformation: a unified approach to shape interpolation and skeleton-driven deformation. In *ACM Siggraph*, pages 165–172, 2000.

[LV99] F. Lazarus and A. Verroust. Level set diagrams of polyhedral objects. In *Proc. of the Symp. on Solid Modeling and Applications*, pages 130–140, 1999.

[Mic86] C. A. Micchelli. Interpolation of scattered data: Distance matrices and conditionally positive definite functions. *Constrained Approximation*, 2:11–22, 1986.

[MKB+08] S. Martin, P. Kaufmann, M. Botsch, M. Wicke, and M. Gross. Polyhedral finite elements using harmonic basis functions. *Computer Graphics Forum*, 27(5):1521–1529, 2008.

[MN03] N. J. Mitra and An Nguyen. Estimating surface normals in noisy point cloud data. In *Proc. of the ACM Symp. on Computational Geometry*, pages 322–328, 2003.

[MPS+04a] M. Mortara, G. Patanè, M. Spagnuolo, B. Falcidieno, and J. Rossignac. Blowing bubbles for multi-scale analysis and decomposition of triangle meshes. *Algorithmica*, 38(1):227–248, 2004.

[MPS+04b] M. Mortara, G. Patanè, M. Spagnuolo, B. Falcidieno, and J. Rossignac. Plumber: a method for a multi-scale decomposition of 3d shapes into tubular primitives and bodies. In *Proc. of the ACM Symp. on Solid Modeling and Applications*, pages 339–344, 2004.

[OBA+03] Y. Ohtake, A. Belyaev, M. Alexa, G. Turk, and H.-P. Seidel. Multi-level partition of unity implicits. *ACM Siggraph*, 22(3):463–470, 2003.

[PCMS04] V. Pascucci, K. Cole-McLaughlin, and G. Scorzelli. Multi-resolution computation and presentation of contour trees. In *Conference on Visualization, Imaging, and Image Processing*, pages 452–290, 2004.

[PKKG03] M. Pauly, R. Keiser, L. P. Kobbelt, and M. Gross. Shape modeling with point-sampled geometry. In *ACM Siggraph*, pages 641–650, 2003.

[PS12] G. Patanè and M. Spagnuolo. Local approximation of scalar functions on 3d shapes and volumetric data. *Computer & Graphics*, (To appear), 2012.

[PSBM07] V. Pascucci, G. Scorzelli, P.-T. Bremer, and A. Mascarenhas. Robust on-line computation of Reeb graphs: simplicity and speed. In *ACM Siggraph 2007*, pages 58.1–58.9, 2007.

[PSF08] G. Patanè, M. Spagnuolo, and B. Falcidieno. Reeb graph computation based on a minimal contouring. In *Proc. of Shape Modeling and Applications*, pages 73 – 82, 2008.

[PSF09] G. Patané, M. Spagnuolo, and B. Falcidieno. A minimal contouring approach to the computation of the reeb graph. *IEEE Transactions on Visualization and Computer Graphics*, 2009.

[Ree46] G. Reeb. Sur les points singuliers d'une forme de pfaff completement integrable ou d'une fonction numerique. In *Comptes rendus de l'Académie des sciences*, pages 847–849. Sciences Park, 1946.

[RU90] S.P. Raya and J.K. Udupa. Shape-based interpolation of multidimensional objects. *IEEE Transactions on Medical Imaging*, 9(1):32 –42, mar 1990.

[SKK91] Y. Shinagawa, T. L. Kunii, and Y. L. Kergosian. Surface coding based on Morse theory. *IEEE Computer Graphics and Applications*, 11:66–78, 1991.

[SNdB02] S. Svensson, I. Nystr om, and G. Sanniti di Baja. Curve skeletonization of surface-like objects in 3D images guided by voxel classification. *Pattern Recognition Letters*, 23(12):1419–1426, 2002.

[SP07] K. Siddiqi and S. M. Pizer, editors. *Medial Representations: Mathematics, Algorithms and Applications*. Springer, 2007.

[SWLG03] R. Stevens, C. Wroe, P. Lord, and C. Goble. *Ontologies in bioinformatics*, pages 635–657. Springer, 2003.

[TGSP09] J. Tierny, A. Gyulassy, E. Simon, and V. Pascucci. Loop surgery for volumetric meshes: Reeb graphs reduced to contour trees. *IEEE Transactions on Visualization and Computer Graphics*, 15(6):1177–1184, 2009.

[TO02] G. Turk and J. F. O'Brien. Modelling with implicit surfaces that interpolate. *ACM Trans. Graph.*, 21(4):855–873, 2002.

[TSK97] S. Takahashi, Y. Shinagawa, and T. L. Kunii. A feature-based approach for smooth surfaces. In *Proc. of the Symp. on Solid Modeling and Applications*, pages 97–110, 1997.

[VGRP+10] G. Vasilakis, A. García-Rojas, L. Papaleo, C. Catalano, F. Robbiano, M. Spagnuolo, M. Vavalis, and M. Pitikakis. Knowledge-based representation of 3d media. *International Journal of Software Engineering and Knowledge Engineering*, 20(5):739–760, 2010.

[WBB+08] D. L. Wheeler, T. Barrett, D. A. Benson, S. H. Bryant, K. Canese, V. Chetvernin, D. M. Church, M. DiCuccio, R. Edgar, S. Federhen, M. Feolo, L. Y. Geer, W. Helmberg, Y. Kapustin, O. Khovayko, D. Landsman, D. J. Lipman, T. L. Madden, D. R. Maglott, V. Miller, J. Ostell, K. D. Pruitt, G. D. Schuler, M. Shumway, E. Sequeira, S. T. Sherry, K. Sirotkin, A. Souvorov, G. Starchenko, R. L. Tatusov, T. A. Tatusova, L. Wagner, and E. Yaschenko. Database resources of the national center for biotechnology information. *Nucleic Acids Research*, 36:13–21, 2008.

[Wen95] H. Wendland. Real piecewise polynomial, positive definite and compactly supported radial functions of minimal degree. *Advances in Computational Mathematics*, 4(4):389–396, 1995.

[WHDS04] Z. Wood, H. Hoppe, M. Desbrun, and P. Schröder. Removing excess topology from isosurfaces. *ACM Transactions on Graphics*, 23(2):190–208, 2004.

[Whi00] R. T. Whitaker. Reducing aliasing artifacts in iso-surfaces of binary volumes. In *Proc. of IEEE Symp. on Volume Visualization*, pages 23–32, 2000.

[WSLG07] O. Weber, O. Sorkine, Y. Lipman, and C. Gotsman. Context-aware skeletal shape deformation. *Computer Graphics Forum*, 26(3), 2007.

[YBS07] S. Yoshizawa, A. Belyaev, and H.-P. Seidel. Skeleton-based variational mesh deformations. *Computer Graphics Forum*, 26(3):255–264, 2007.

[YHMY08] H.-B. Yan, S. Hu, R. R. Martin, and Y.-L. Yang. Shape deformation using a skeleton to drive simplex transformations. *IEEE Transactions on Visualization and Computer Graphics*, 14(3):693–706, 2008.